

## Mixed effects modelling for glass category estimation from glass refractive indices

---

### Abstract

520 glass fragments were taken from 105 glass items. Each item was either a container, a window, or glass from an automobile. Each of these three classes of use are defined as glass categories. Refractive indexes were measured both before, and after a programme of re-annealing. Because the refractive index of each fragment could not in itself be observed before and after re-annealing, a model based approach was used estimate the change in refractive index for each glass category. It was found that less complex estimation methods would be equivalent to the full model, and were subsequently used. The change in refractive index was then used to calculate a measure of the evidential value for each item belonging to each glass category. The distributions of refractive index change were considered for each glass category, and it was found that, possibly due to small samples, members of the normal family would not adequately model the refractive index changes within two of the use types considered here. Two alternative approaches to modelling the change in refractive index were used, one employed more established kernel density estimates, the other a newer approach called log-concave estimation. Either method when applied to the change in refractive index was found to give good estimates of glass category, however, on all performance metrics kernel density estimates were found to be slightly better than log-concave estimates, although the estimates from log-concave estimation possessed properties which had some qualitative appeal not encapsulated in the selected measures of performance. These results and implications of these two methods of estimating probability densities for glass refractive indexes are discussed.

*Keywords:* evidence evaluation, likelihood ratio, re-annealing, refractive index, glass, glass category, MCMC, kernel density, log-concave, ECE, mixture model

# 1. Introduction

Glass is a material that is associated with many areas of human activity. In buildings it appears most frequently as window glass, in automotive transport it forms windows and windscreens, headlamps, mirrors and light bulbs. In a domestic setting it makes up windows and light bulbs, bottles, jars, tableware and decorative items. Fragments of glass with a maximum measurement, in any linear dimension, equal to, or less than, 1 millimetre can be formed during events such as car accidents, burglaries, and fights. These fragments may be recovered from the scene of the incident, as well as the clothes, and body, of participants in any event of forensic interest, and can be employed to provide evidence of activity [1, 2] as well as source [1, 3–7].

## 1.1. Refractive index measurements

The measurement of refractive index is frequently conducted on glass fragments using a thermo-immersion method. If the amount of material which is available for analysis is large enough, that is greater than 0.5 mm, the fragment may be divided into at least two small particles, each of which can have their refractive indexes measured.

Fragments of glass can also be annealed. During annealing tensions present in the glass object are removed. Stresses occur in glass because of the limited thermo-conduction of glass, which means that the outer glass layers can cool significantly faster than the inner layers [8]. This effect leads to the establishment of internal stresses during the manufacturing process. The stresses take the form of compression in the outer layers, and the inner layers are subject to tearing forces [8], and have an influence on the value of the refractive index.

Annealing will eliminate or reduce internal stresses in glass. The annealing process works in such a way that the stresses between the inner layers of the glass are removed slowly during controlled heating at high temperature. Afterwards slow cooling is carried out to allow the glass layers to relax to states in which the internal/external stresses are minimised.

Re-annealing, the term used here to refer to a secondary annealing process for forensic purposes, is often undertaken in a muffle furnace, the heating/cooling program can

vary depending upon the glass, and preferences of the individual scientist. A typical temperature program [8–12] contains a step of fast heating up to 550°C, called the maximum temperature, and it is the temperature at which most glass objects begins to melt, and then the glass fragment is kept at this temperature for some pre-determined period in order to eliminate those stresses present in the glass. In British laboratories, short temperature programs for re-annealing are conducted in tube furnaces. The glass fragment is heated up to 590°C, kept at this temperature for 12 minutes and then cooled at a rate of 4.5 °C/min down to 425°C at which it is held for one minute before being cooled down to room temperature [9]. Long temperature programs can be used which employ fast heating of the specimen up to a high temperature, but this temperature is retained for a longer time; typically 10 to 15 hours, before the glass is slowly cooled down.

The literature offers little agreement as to which of the temperature programmes are best suited to estimating the change in refractive index [8, 10–13]. Marcouiller [12] used a programme which took 28.5 hours and showed that this long temperature programme allowed a clear distinction between toughened and non-toughened glass objects. It has also been shown [11, 13, 14] that shorter temperature programs, in some cases as short as an hour [11], allow differentiation between toughened and non-toughened glass. However some of these conclusions have been contradicted by Newton *et al.* [8], where a categorical discrimination between toughened and non-toughened glass could not be made using a short temperature programme. Nevertheless, it is clear that change in refractive index with a suitable re-annealing programme can be employed as an observation upon which to base some form of a classification of glass [8, 12, 15]

Commonly produced glass types such as building windows, and container glasses, are often annealed as part of the manufacturing process. However, some glass types are not annealed at all, and in others stresses are deliberately introduced as part of a toughening process, for example toughened glass which is used for car windows and cupboard doors.

For the toughened glasses, differences between refractive index values measured after re-annealing (RIa), and those observed before the re-annealing process (RIb), should be larger than differences for non-toughened glasses. This is because a higher degree of structural stresses, which were introduced into the glass object during the toughening

process, are removed during the re-annealing process. These differences in manufacturing methods mean that the change in refractive index brought about by deliberate annealing ( $\Delta RI = RI_a - RI_b$ ) can be used to distinguish between toughened and non-toughened glasses [8, 16].

## 2. Materials and methods

### 2.1. The glass sample

The refractive index was measured for a sample of 105 glass items. Each item had either four, or six, fragments observed both before, and four, or six, fragments observed after re-annealing. Each glass object was selected from one of three glass use categories, these categories were: automotive glass, 32 items; window glass, 23 items; and container glass, 50 items. The measurements were made at the Institute of Forensic Research, Krakow [17, 18].

### 2.2. Refractive index measurement

The refractive index of the glass fragments was measured using the GRIM 2 set (Foster & Freeman Ltd., United Kingdom), which contains a microscope with phase contrast (Leica, Germany), digital camera (Sony, Japan), heating stage (Mettler, Toledo, Spain), computer and GRIM analyser. Measurements were taken at 589nm. Measurements of the refractive index before ( $RI_b$ ) and after ( $RI_a$ ) re-annealing were made on such way that each glass fragment was covered with silicone oil (silicone oil B, Foster & Freeman Ltd., United Kingdom) and broken to obtain suitable edges for the measurement process.

It was not possible to recover glass fragments of such a size that a measurement of the refractive index could be made, then the fragment annealed, and the refractive index measurement repeated to yield two measurements for that fragment. So different glass fragments from the same object were divided into two sub-fragments, both having the refractive index measured, however one fragment was annealed before the refractive index was measured.

The refractive index was calculated from a calibration function which comprised 13 (B1-B13) observations from different known glass standards supplied by the producer

of the GRIM 2 set (Foster and Freeman Ltd., UK). Each standard was measured 5 times. The quality of measurement were also checked by analysis of B8 standard on each day when refractive index observations made. The match temperature ( $\tau$ ) is the temperature when the refractive index of the immersion oil and the refractive index of the glass fragment are equal. A linear calibration function was calculated by least squares methods ( $RI = 1.5434 - 0.0004\tau$ ). The Pearson correlation coefficient was  $r \geq 0.9999$ , which suggests that the calibration function adequately describes the linear dependency between the refractive index and the match temperature  $\tau$ .

### 2.3. Annealing procedure

The re-annealing process was conducted using a muffle furnace (Nabertherm L3/11 with a P320 programmer unit, Germany). A short temperature program was used. The furnace was heated to 650°C over a period of 35 minutes, and then heated up to 700°C in a further 10 minutes. A slow cooling period then began, decreasing the temperature down to 300°C over the next 2.5 hours. The glass fragments were put into a metal sample holder. The temperature of the metal sample holder was measured by a thermocouple (Fluke 54 II, K type, USA).

### 2.4. Calculation of $\Delta RI$

Let each observation of refractive index be denoted  $x_{ijkl}$  where the suffix indicates is the known glass category, where  $i \in \{\text{automotive, container, window}\}$ , the suffix  $j$  indicates the re-annealing status so that  $j = \{\text{before, after}\}$ . The suffix  $k$  is the item for the  $i^{\text{th}}$  type in the  $j^{\text{th}}$  re-annealing state, such that  $k \in \{1, 2, \dots, m_i\}$ ,  $m \in \{32, 23, 50\}$ , and the suffix  $l$  indicates the  $l^{\text{th}}$  replicated observation on the  $k^{\text{th}}$  item, from the  $i^{\text{th}}$  glass category, in the  $j^{\text{th}}$  re-annealing state, such that  $l \in \{1, 2, \dots, q\}$ . In the case of the samples used in this work  $q_{ij} \in \{4, 6\}$ .

The replicated observations for the  $k^{\text{th}}$  item from the  $i^{\text{th}}$  type cannot be considered paired as, due to the small size of the fragments after breakage, it was not possible to observe refractive index upon the same fragment of glass both before, and after re-annealing. Thus, if before re-annealing can be abbreviated as  $b$ , and after re-annealing as  $a$ , there is no requirement for  $q_{ib} = q_{ia}$ . There is also no particular reason why there

should be the same number of items observed for each glass category, however, it is necessary that each and every item has a sample of refractive index observations made for each re-annealing state.

In the case here, for each item, equal numbers of refractive index observations were made before, and after, re-annealing, although the number of refractive index observations varied between items. As for each item  $q_{jbbk} = q_{jakk}$  the differences between the mean refractive index observations ( $\Delta RI_j$ ) between the two re-annealing states could be calculated:

$$\Delta RI_j = \frac{1}{q_{jk}} \left( \sum_l^{q_{jk}} x_{iakl} - \sum_l^{q_{jk}} x_{ibkl} \right) \quad (1)$$

Here the difference is defined as the observations in refractive index made after re-annealing, minus those observations made before re-annealing. There is no particular significance to the ordering of the two terms in the difference, a reverse ordering will simply lead to the negation of the resultant difference.

## 2.5. Estimation of $\Delta RI$ within each glass category

If the respective  $\Delta RI_j$ 's are considered for each of the  $n$  use types the following box and whiskers plot can be drawn:

From Figure 1 the utility of  $\Delta RI$  as some useful means by which to distinguish fragments of glass drawn from automotive, window, and container glass, is clear.

What is also clear-cut is that the  $\Delta RI$ s on the whole, for window glass, seem to be negative relative to both automotive and container glass. It is this apparent decrease in refractive index with re-annealing which may prove contentious to scientists who are professionally concerned with glass. Due to the potentially controversial nature of this observation, and the technical difficulties in making estimates for  $\Delta RI$ , it was considered necessary to deploy model based methods to calculate the most appropriate estimates for the  $\Delta RI$  for each glass category.

Assume that, for the wider population of observations, each observation, from each fragment, is independent and identically distributed (**iid**) normal given the item and state of re-annealing, and can be parametrised:

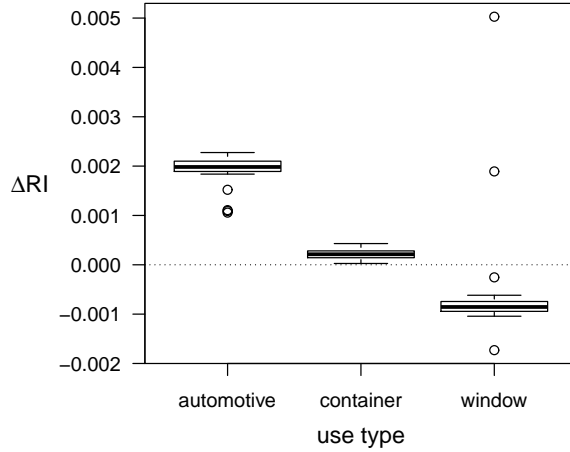


Figure 1: Box and whiskers plot of the difference in the means of refractive index ( $\Delta RI$ ) for each of the three glass use types. The difference is taken as the mean refractive index observed from fragments from a glass object which have been annealed, minus, the mean refractive index observed from fragments from the same glass object, the fragments not having been annealed.

$$x_{ibkl} \sim N(\mu_{ibk_i}, \sigma_b^2)$$

$$x_{iakl} \sim N(\mu_{iak_i}, \sigma_a^2)$$

where a single variance term is used for all replicates from all items, however there is a separate variance term for each state of re-annealing.

The mean for all fragments for each item after the fragments have been annealed can be written as:

$$\mu_{iak} = \mu_{ibk} + \beta_{ik} + \epsilon$$

$$\beta_{ik} \sim N(\mu_i, \sigma^2)$$

$$\epsilon \sim N(0, \sigma_\epsilon^2)$$

where  $\mu_{ibk}$  is a fixed effect term for the mean of un-annealed refractive index observations for each item, but is of no interest in itself. The  $\beta_{ik}$  term is a random effect due to each individual item, and the effect of re-annealing upon that item. The mean refractive index difference for each item  $\beta_{ik}$  can be assumed to be distributed normal

Table 1: Summary information for the model given in Appendix A. The simulations sampled some 31,000 values from the posterior distribution of each value of  $\mu_i$ . The first 1,000 values being discarded. Given for comparison in the the second two columns are equivalents to those parameters calculated using a general linear model of  $\Delta\text{RI}$  as a response to glass category.

category	mcmc		glm	
	$\mu_i$	se	$\Delta\text{RI}_i$	se
automotive	0.00192	0.00013	0.00192	0.00012
container	0.00022	0.00010	0.00022	0.00015
window	-0.00050	0.00015	-0.00050	0.00018

with parameters  $\mu_i$  and  $\sigma^2$ ;  $\epsilon$  is a pure error term. The  $\mu_i$  terms are the main focus of this part of the investigation, and can be considered fixed terms in the model due to the influence of glass category upon the change in refractive index.

The parameters  $\mu_i$  were estimated using Gibbs sampling and standard software [19–21]. Details are given in Appendix A.

The simulations were run repeatedly using a variety of initial values for each parameter. Given the model described in Appendix A all chains sampled for each parameter  $\mu_i$  were consistent with one another, showed good mixing, with little auto-correlation at any of the observed levels of lag. The estimates are samples from the posterior distributions of  $\mu$ , summaries are presented in Table 1.

The mean values given in Table 1 are given alongside values estimated from a general linear model fitted to  $\Delta\text{RI}$  for each glass category. Thus  $\Delta\text{RI}$  and  $\mu_i$  can be regarded as equivalent parameters. The two sets of parameter estimates are very similar, indicating that in practice the complicated mixed model outlined in Appendix A can be closely approximated by a far simpler model which simply uses  $\Delta\text{RI}$  calculated from Equation 1.

### 3. Glass category estimation

Having established that the change in refractive index,  $\Delta\text{RI}$ , varies systematically between the three use types represented in this sample, and that the differences between

estimating  $\Delta\text{RI}$  as the differences between the means of the observations, and more complicated model based methods of estimating  $\Delta\text{RI}$ , it would seem appropriate to use  $\Delta\text{RI}$  as an observation upon which to base some estimate of the glass category of any glass item for which the glass category was unknown.

### 3.1. The evidential value of glass category

Evidence of use-type for glass may be used as part of the formal evidential process, and presented as such in a court, or may be employed in a less formal intelligence role. If the latter then it could be that the fact finder may be happy to use a posterior probability for any recovered fragment of any glass from an item of unknown glass category is of any specific glass category [22]. However, as the prior odds are all that is needed to change a likelihood ratio [5] to a posterior probability, the focus of the rest of this paper shall be upon the calculation of a likelihood ratio as a measure of *strength of evidence* for glass category as this is the more general of the two.

Zadora [16] reviewed several methods of use classification, including a multivariate kernel density approach. This work employed observations on both the refractive index, and the major, and minor, elemental composition to assign, using a variety of classification measures, including an adaptation of a kernel based multivariate likelihood ratio first developed by Aitken *et al.* [5–7]. Here we focus upon developing, and exploring some of the options for, a simpler means of treating univariate observations of  $\Delta\text{RI}$ .

Aitken & Taroni [23] express the likelihood ratio in favour of proposition  $H_p$ , given by evidence  $E$  as:

$$\text{LR}_{H_p} = \frac{\Pr(E|H_p, I)}{\Pr(E|H_d, I)}$$

where  $H_p$  and  $H_d$  are propositions put forward by the prosecution and defence respectively.  $I$  can be any background information germane to the propositions under consideration.

In this instance the evidence  $E$  is some change in refractive index estimated for some item, or fragment from some item, of an unknown glass category; denote the glass item of unknown glass category  $y$ , and the change in refractive index  $\Delta\text{RI}_y$ . The propositions  $H_p$  and  $H_d$  then refer to whether  $y$  was a member of some specific use group  $r$ , or some

use group other than  $r$ . The likelihood ratio in favour of  $y$ 's membership of use group  $r$  can then be written:

$$\text{LR}_{H_p} = \frac{\Pr(\Delta\text{RI}_y | y \in r, I)}{\Pr(\Delta\text{RI}_y | y \notin r, I)} \quad (2)$$

In practice the distribution of  $\Delta\text{RI}$  for any glass category  $r$  will be estimated from a sample of similar  $\Delta\text{RI}$  observations from glass objects of glass category  $r$ .

### 3.2. Distributional form of $\Delta\text{RI}$

Figure 2 is a qq-plot for each glass category from the sample of  $\Delta\text{RI}$ s shown in Figure 1.

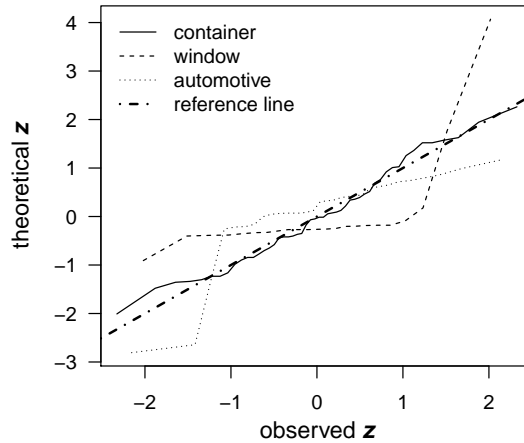


Figure 2: Quantile-quantile plot for the values of  $\Delta\text{RI}$  for each use group. Each set of  $\Delta\text{RI}$  has been standardised. The dot-dash line is a reference line indicating the most likely location for truly **iid** normal variates. There is little evidence to support the notion that the distribution of  $\Delta\text{RI}$  for any use group, other than container glass, is normal.

With the exception of those  $\Delta\text{RI}$ s from containers it is unlikely that the  $\Delta\text{RI}$  observations for windows, and automotive glass, from this particular sample will be **iid** normal. This may be a consequence of small samples for both automotive glasses, and window glasses, and may seem at odds with the assumption of normality made to calculate the values in Table 1, however, it should be borne in mind that this assumption was for the individual observations of  $RI_b$  and  $RI_a$ , and not for  $\Delta\text{RI}$ , and although one might expect the distribution of the difference between two random variables, both of which

are normally distributed, to itself be normal, it appears not to be the case from the small samples studied in this work.

Here two approaches to the estimation of the probabilities needed for Equation 2 will be considered for the distribution of  $\Delta\text{RI}$ :

1. **Kernel density estimation** - which has been described as a “sum of bumps” derived from the data [24, 25]. In this instance the numerator for Equation 2 can be written:

$$\Pr(\Delta\text{RI}_y|y \in r, I) = \frac{1}{m_r} \sum_j^{m_r} \mathbf{K}(\Delta\text{RI}_y, h_r)$$

where  $m_r$  is the sample size of glass objects for the specific glass category  $r$ .  $\mathbf{K}$  is some kernel function [24], and  $h_r$  a smoothing parameter to that function. Here the kernel function for each glass category will be normal, with plug in band width  $h_i$ , being given as  $h_i = (4/3)^{(1/5)} m_i^{-(1/5)} \sigma_i^2$ , the  $\sigma_i^2$  term being the variance in  $\Delta\text{RI}$  for the  $i^{\text{th}}$  glass category.

The denominator is written in a similar fashion, except the density would be summed over each glass category in the sample not including  $r$ :

2. **Log concave estimation** - is a way by which the empirical density for any **iid** random observations can be approximated using maximum likelihood methods. The caveat is that the true distribution must belong to the family of concave distributions, which most commonly employed uni-variate, and multi-variate do. Log-concave estimation strongly implies unimodality for the distribution, although an advantage is that there is no smoothing parameter to estimate, the estimation being said to be in some sense “automatic”. If a kernel density estimate is akin to estimating a density by throwing handfuls of probability at the sample space of interest, log concave estimation is like the erection of a sequence of “tent poles”<sup>1</sup> across the same space to achieve the same effect.

The process of log-concave fitting is algorithmic, and a fuller description can be found in the work of Cule *et al.* [26]. The estimation algorithm used was that of the **logcondens** in the library for **R** [27].

---

<sup>1</sup>Samworth *pers. comm.*

Using log-concave estimation the numerator for Equation 2 can be written:

$$\Pr(\Delta RI_y | y \in r) = C_r(\Delta RI_y)$$

where  $C_r$  is the log concave estimate for the density of  $\Delta RI_y$  for the use group in question,  $r$ . As log-concave estimation strongly implies unimodality, and, from Figure 1, it is unlikely that several groups can properly modelled using any distribution with a single mode, the denominator was calculated as the sum of components contributed by all non  $r$  use types, and is a form of mixture model for the background probability. Thus:

$$\Pr(\Delta RI_y | y \notin r) = \frac{1}{n-1} \sum_i^n C_i(\Delta RI_y) \quad : i \neq r$$

Plots for the calculated probability density functions for  $\Delta RI_i$  are given in Figure 3. Figure 3a shows kernel density estimates, and Figure 3b log concave estimates. What is apparent from Figure 3 is that in the extremes for the kernel density estimates for, for example, the density of  $\Delta RI$  for container and automotive glass, where are few observations, the density varies considerably. This is not the case for the log concave estimates, which appear more stable in these regions.

### 3.3. Discussion

Likelihood ratio values were calculated for each glass item in the sample using both kernel density estimates, and log-concave estimates under the propositions

- $H_p \equiv$  the item was of use group  $r$ ,
- $H_d \equiv$  the item was of any group other than use group  $r$ .

The likelihood ratio values for the membership for each glass item are given in the table in Appendix B.3, along with their known glass category.

The discrepancy between those likelihood ratios calculated using log-concave estimation, and those calculated using kernel density estimation, is entirely due to the behaviour in the low density regions of the estimated functions. This effect operates across all values of the  $\Delta RI$  spectrum as, from Figure 1, the three groups of glass category represented

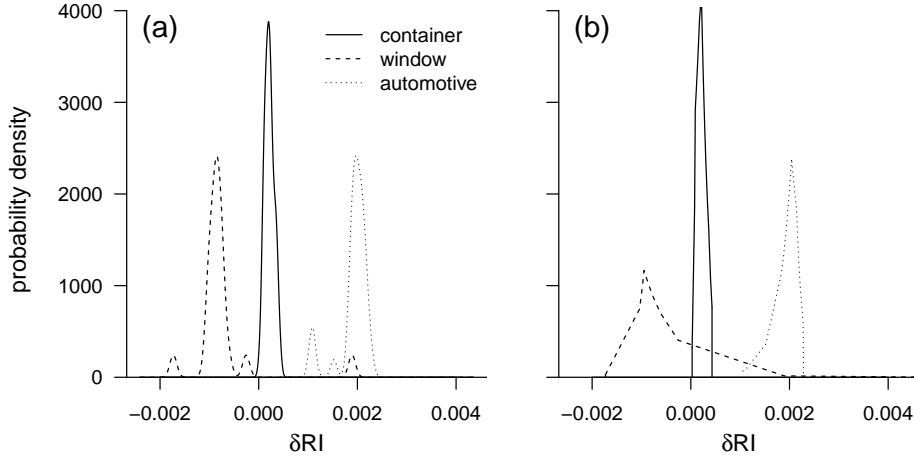


Figure 3: Probability density estimates for (a) kernel density methods, (b) log concave estimation. Both (a) and (b) share a vertical scale. The log concave estimates appear more stable, compared to the kernel density estimates, in the extreme regions of their densities.

here are quite highly separated. For example if one considers an observation which is truly from window glass, and its  $\Delta RI$  value is fairly central to the distribution of window  $\Delta RIs$  at about 0.0001, then the corresponding density is relatively large, and well known. However, the sum of the densities for that same  $\Delta RI$  were it from an automotive source, or container source, may be very small. This leads to a high likelihood ratio, which is what one would expect given that this hypothetical example  $\Delta RI$  is truly from a window. However the magnitude of the likelihood ratio is entirely given by the estimate of these small densities which are in the tail end of their respective density functions, and about which least is known as it is in these tail densities fewest observations exist.

Figure 3 shows the differences between the densities estimated by kernel density methods and those estimates made log-concave estimation. In the light of the foregoing discussion, and the seeming greater stability of the densities made by log-concave estimation in the tail ends of  $\Delta RI$  for each use group, it is easy to see why likelihood ratios made by log-concave estimation tend to be lower and less variable.

Those likelihood ratios from glass items known to be from containers, as expected, tended to be low for the propositions that those items were truly from automotive or window sources, and higher for the proposition that the item was from a container.

Overall the high likelihood ratios tended to be lower when calculated using log-concave estimations methods then kernel density techniques.

Likelihood ratios from items known to be from window glass are all infinite when log-concave estimates are used to calculate the likelihood ratios, and again very high when kernel density methods are used. A further inspection of the calculations showed that the infinite values given by log-concave estimation is due to the fact that many of the  $\Delta$ RI's from the window group fell outside the range of  $\Delta$ RI for either of the other groups. One of the properties of log-concave estimation is that any value outside the concave hull of the estimated distribution function is zero [26]. As, in many of the cases for window glass, the denominator for the likelihood ratio was zero, the likelihood ratio is therefore infinite.

A similar pattern is seen where those likelihood ratios from glass known to be from automobiles are, expectedly, higher for propositions revolving around a automobile based source then for a window, or container based source. Again the magnitude of the differences between log-concave and kernel density estimates is apparent, as is the variation in the magnitudes.

### 3.4. Relative performances

A brief inspection of Table 2 would suggest a false positive rate of about 2%, and a false negative rate of  $\approx 1.4\%$ , for likelihood ratios calculated using log-concave estimation. If the likelihood ratios are calculated using kernel density methods a false positive rate of about 0.3%, and a false negative rate of about 1.2%. However, this would be using a rather simplistic notion of glass category assignment. Were a less naive approach which made glass category assignments based on moderate evidence, say likelihood ratios in the 0.1 to 10 range deemed to be of so little evidential value as to be inconclusive, then the false positive rate for log-concave estimation would fall to about 0.3%, with a false negative rate of  $\approx 1.3\%$ . For kernel density estimation the false positive rate would remain unchanged, and the false negative rate fall to about 0.3%. However, were this the case then many items could not be conclusively assigned to a glass category (Table 2); forensically though, non-assignment due to a lack of certainty would be of little importance.

The above treatment of likelihood ratios as some measure upon which to base a classification can be useful, especially given that  $\Delta\text{RI}$  may be used in intelligence, it is however, not the primary purpose of a measure of evidential worth which seeks to evaluate the extent to which observations can be said to support, or contradict, any given proposition. Ramos [28] used a more nuanced approach based upon cross-entropy to evaluate likelihood ratios for dichotomous propositions.

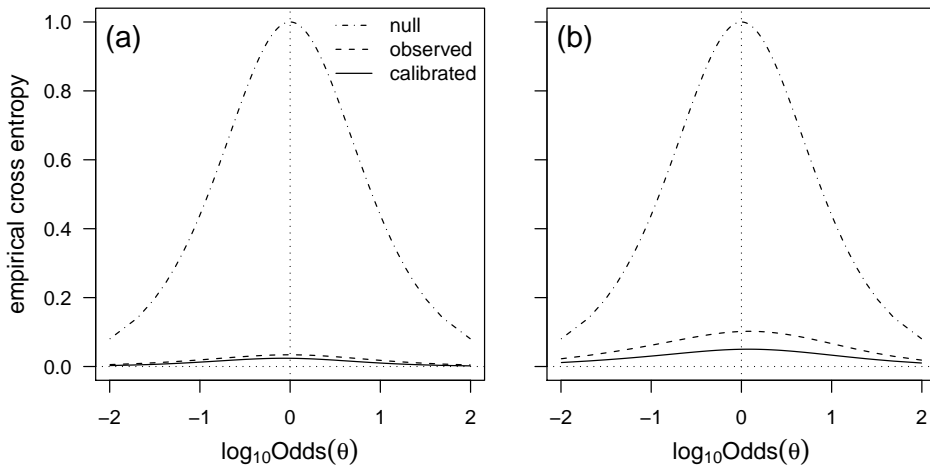


Figure 4: Empirical cross-entropies for likelihood ratios made by (a) kernel density methods, (b) log concave estimation. Both (a) and (b) share a vertical scale. Each sub-figure has three lines plotted. The first line (dot-dashed) is a line representing the *null* cross-entropy. This is the cross entropy where the observations are giving no information about the propositions under examination, and are when each likelihood ratio is equal to 1. The second line (dashed) is the cross-entropy given by the recorded observations. The final line (solid) is an ideal line calibrated from theory. The better the empirical values of cross-entropy resemble the theoretically derived values of cross-entropy, and the less the values resemble those values from the *null* cross-entropy, the more information the observations contain about the propositions under consideration.

Empirical cross entropy is a measure of *information*, and considers not only whether a decision based upon some statistic, such as a likelihood ratio, makes the right decision, but the costs of wrong, and benefits of correct, decisions. It is a matter for intuition that classifying some glass item as automotive glass when it is container, or window, glass is in error, and it is obvious that a strong classification would lead to a higher potential cost than a weak classification. Empirical cross-entropy uses the strengths of the assignments

from the calculated likelihood ratios for a set of items of known origin. It compares these strengths to two theoretical situations:

1. where the observations carry absolutely no information about the origins of any fragment of glass under consideration.
2. Where the strengths of assignment have been calibrated to produce a set of cross-entropies which represent some idealised measure of evidential value for the set of observations under consideration.

The empirical cross-entropies calculated from the observed likelihood ratios can then be compared to these other two theoretical cross-entropies, and some assessment can be made of how much information the underlying system of assignment as to the source of any glass fragment. A peculiarity is that the calculation of empirical cross-entropy can only be made for a known prior, so the technique employed by Ramos [28] is to use a range of prior probabilities for the glass category of each class item. These prior probabilities are expressed in a  $\log(\text{Odds})$  form in the empirical cross-entropy plots, and is reflected in Figure 4.

Figure 4 shows the empirical cross-entropies calculated from the likelihood ratios for both kernel density based estimates of the likelihood ratio (Figure 4a), and log-concave estimation (Figure 4b). Likelihood ratios calculated from kernel density estimates clearly offer more information about the glass category of these glass objects, however, both log-concave, and kernel densities estimates, offer a considerable amount of information about glass category.

## 4. Conclusions

Annealing induced changes observed in the refractive index of glass fragments can be used to make inferences about the glass category of the object from which any given fragment was derived. It is clear that for automotive glass the refractive index increases slightly with re-annealing, and for window glass the refractive index decreases. The refractive index of container glasses are nearly unchanged with re-annealing, having, if anything a very slight increase. The negative  $\Delta RI$  values occur when the cooling part of the re-annealing program is faster than the cooling part of the production process of the

glass. Here the stresses built into the glass increase and the refractive index decreases. This could happen when a short re-annealing program is used, or extremely slow cooling rate is used during the production of special glasses such as optical glasses.

Although in detail the measurement of the change in refractive index is made complicated by the fact that it is not possible to observe the refractive index of a small glass fragment both before, and after re-annealing, the difference in the means of two samples of observations, one sample observed before re-annealing, one after re-annealing, can be used as a close approximation to a more complicated model based approach, the differences only being apparent at the sixth decimal place.

The difficulties inherent in glass category estimation have been exacerbated by the distribution of the change in refractive index for any given glass category. Here we have used relatively small samples for each glass category, and it could be that as larger samples become available the distributional form can be adequately modelled by a density function from the normal family of distributions. That has not been the case here, and consequently a resort has had to be made to two different methods of non-parametric estimation. For any performance metric, whether simple measures of false positives and negatives, or the information theoretic based empirical cross entropy, Kernel density methods seem to give better assignments of glass category than log-concave based estimates. However, examination of the form of the densities involved, and the consequent likelihood ratios, leave the observer with a sense of incredulity. Values of up to  $10^{17}$  seem rather high for what is a single univariate observation, and the variability of the likelihood ratios, despite being explicable, seems strange as there is a strong expectation that observations which are similar in the measurement space should form similar evidential values. For any specific glass item those likelihood ratios from log-concave estimation are, with the exception of window glass, far lower than those calculated by kernel density estimation.

To many glass experts the lower, and more uniform, values offered by log-concave estimation may seem much more reasonable. However, unlike an exercise in calibration, where the response may be continuous, the investigator has little idea about any true value of the observations in the light of the propositions of glass category. The investigator's knowledge is limited to whether or not some item is in fact from a specific glass

category, and it is from this dichotomous response used to make some deductions about a continuous measure of evidential value. The inability to make inferences about evidential value from a known classification may be due to the nature of the tools employed to do so. Unless the forensic question revolves solely around assignment of glass category, then reporting of simple false positives and false negatives will be insufficient, as it is usual for forensic questions to be concerned with “how sure”, and “what is the evidence for” some proposition related to glass category. Empirical cross-entropy measures of performance may overcome many of the crudities inherent in dichotomising a continuous measure, however, again here they clearly favour density estimates.

The small number of use types represented in this work may give a misleading impression of how well the re-annealing of glass fragments can be used to make inferences about glass category. It is expected that as more and more glass types are represented the full spectrum of refractive index change will become represented, rather than the relatively discrete measurements seen in Figure 1, and that the likelihood ratios calculated using kernel density methods will become lower simply due to a higher density in the denominator of the likelihood ratio.

The same will be true when a finer taxonomy of glass object is employed. For instance, the forensic question may revolve around some particular jar type, rather than the generic “containers”. In this case it may be that any specific container type will, for glass truly of that type, get high likelihood ratios, providing evidence of membership of that class. However, it could equally be that calculated likelihood ratios would be as large for any other specific container type, and in that case it would be important for the glass expert to realise this was the case before reporting the evidence for the specific type. This is though a matter for the taxonomies adopted by the individual glass expert, and will vary dependent upon the glasses in their particular geographic location.

It is not new to say that change in refractive index with re-annealing contains glass category information, and would be a valuable feature to examine to make some estimate of the glass category, but it is more difficult to make specific recommendations about the number of classes which may be optimal for forensic glass experts to employ. Even making some suggestions about an optimal way to model the conditional distributions for refractive index change is fraught with difficulties. It may eventually be the

case that for any large class of glass objects the distribution of refractive index changes with re-annealing might be best modelled with some member of the normal family, thus simplifying the whole process.

## Acknowledgements

The authors should like to acknowledge the suggestions made by two anonymous referees for the improvement of this paper.

## References

- [1] J. Curran, T. N. Hicks, J. Buckleton, *Forensic Interpretation of Glass Evidence*, CRC Press, 2000.
- [2] R. Cook, I. Evett, G. Jackson, P. Jones, J. Lambert, *Science & Justice* 38 (1998) 151–156.
- [3] J. Curran, C. Triggs, J. Almirall, J. Buckleton, K. Walsh, *Science & Justice* 37 (1997) 241–244.
- [4] J. Curran, C. Triggs, J. Almirall, J. Buckleton, K. Walsh, *Science & Justice* 37 (1997) 245–249.
- [5] C. Aitken, D. Lucy, *Applied Statistics* 53 (2004) 109–122.
- [6] C. Aitken, D. Lucy, G. Zadora, J. Curran, *Computational Statistics and Data Analysis* 50 (2006) 2571–2588.
- [7] C. Aitken, G. Zadora, D. Lucy, *Journal of Forensic Sciences* 52 (2007) 412–419.
- [8] A. Newton, L. Kitto, J. Buckleton, *Forensic Science International* 115 (2005) 119–125.
- [9] B. Caddy, *Forensic examination of glass and paint. Analysis and interpretation*, Taylor & Francis, London, 2001.
- [10] A. R. Casista, P. M. L. Sandercock, *Journal of Canadian Society of Forensic Science* 27 (1994) 171–177.
- [11] J. Locke, R. Winstanley, L. Rockett, C. Ryderd, *Forensic Science International* 29 (1985) 247–258.
- [12] J. Marcouiller, *Journal of Forensic Sciences* 35 (1990) 554–559.
- [13] R. Winstanley, C. Rydeard, *Forensic Science International* 29 (1985) 1–10.
- [14] S. Ryland, *Journal of Forensic Sciences* 31 (1986) 1314–1329.
- [15] M. Underhill, *The annealing of glass. Notes for caseworkers*, Technical Report, Metropolitan Police Forensic Science Laboratory, Aldermaston, London, 1992.
- [16] G. Zadora, *Journal of Forensic Sciences* 54(1) (2009) 49–59.
- [17] M. Pawluk-Kolc, J. Zigba-Palus, A. Parczewski, *Forensic Science International* 174 (2008) 222–228.
- [18] G. Zadora, D. Wilk, *Problems of Forensic Science* 8 (2009) 365–385.
- [19] D. Spiegelhalter, A. Thomas, N. Best, W. Gilks, *BUGS: Bayesian inference using Gibbs Sampling*, Version 0.5., MRC Biostatistics Unit, Cambridge, 1995.
- [20] D. Spiegelhalter, A. Thomas, N. Best, D. Lunn, *WinBUGS: User Manual*, Version 2.10., Medical Research Council Biostatistics Unit, Cambridge, 2005.

- [21] A. Thomas, B. O'Hara, U. Ligges, S. Sturtz, *R News* 6 (2006) 12–17.
- [22] D. Lucy, *Age Estimation in the Living: the Practitioners Guide*, John Wiley & Sons, pp. 267–283.
- [23] C. Aitken, F. Taroni, *Statistics and the Evaluation of Evidence for Forensic Scientists*, Wiley, 2004.
- [24] B. Silverman, *Density Estimation for Statistics and Data Analysis*, Chapman and Hall, London, 1986.
- [25] M. Wand, M. Jones, *Kernel Smoothing*, Chapman & Hall, London, 1995.
- [26] M. L. Cule, R. J. Samworth, M. I. Stewart, *Journal of the Royal Statistical Society Series B* (2010).
- [27] K. Rufibach, *Journal of Statistical Computation and Simulation* 77 (2007) 561–574.
- [28] D. Ramos, J. Gonzalez-Rodriguez, *Odyssey-2008* (2008).

## Appendix A. Model for $\Delta$ RI

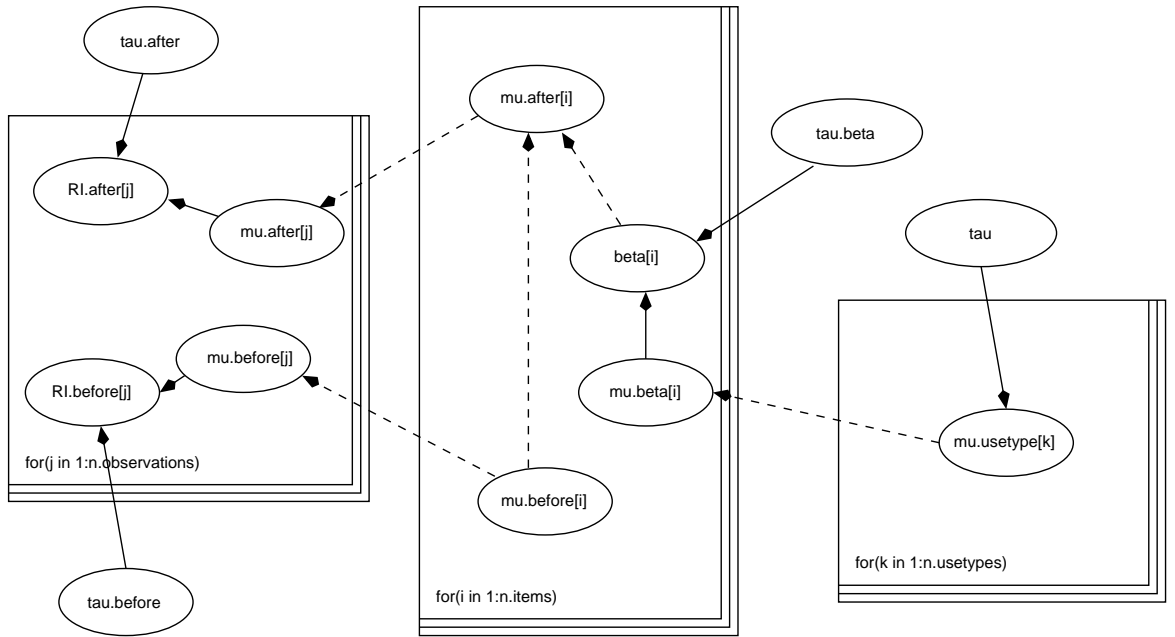


Figure A.5: OpenBUGS doodle of the model described in the text. The notation differs from that in the text as the requirements for names in OpenBUGS, or any BUGS language [20], is different to that possible in mathematical notation. In a change from DoodleBUGS conventions, edges leading to logical nodes are represented as dashed lines with arrows, rather than closely set parallel lines with arrows.

The model represented as a graph above can be notated:

```

model{
  for(j in 1 : n.observations)
  {
    RI. after [j] ~ dnorm(mu. after [j] , tau. after )
  }
}

```

```

    RI.before[j] ~ dnorm(mu.before[j], tau.before)
    mu.after[j] <- mu.after[item[j]]
    mu.before[j] <- mu.before[item[j]]
  }

for(i in 1 : n.items)
  {
    beta[i] ~ dnorm(mu.beta[i], tau.beta)
    mu.beta[i] <- mu.group[group[i]]
    mu.after[i] <- mu.before[i] + beta[i]
    mu.before[i] ~ dnorm(0.0, 1.0E-6)
  }

for(k in 1 : n.groups)
  {
    mu.group[k] ~ dnorm(0.0, tau)
  }

tau.after ~ dnorm(2.0E+6, 1.0E-6)
tau.before ~ dnorm(2.0E+6, 1.0E-6)
tau.beta ~ dnorm(2.0E+6, 1.0E-6)
tau ~ dgamma(2.5, 2.5)
}

```

The only unusual feature is the use of prior distributions for some of the precisions which are normal with large location, and vague, rather than the more usual gamma prior. The idea was to sample from a vague, but positive space for these precision elements. Unfortunately due to the very small variances involved, for example the marginal variance for the refractive indexes is in the order of  $6 \times 10^{-6}$ , or a precision of  $1.5 \times 10^5$ , a more conventional prior, for example  $\Gamma(2.5, 2.5)$ , would not allow the algorithm to sample from

anything like a realistic portion of the possible space in which these variances exist. So a compromise vague prior, with large location was selected to enable sampling from the appropriate section of the variance space.

## Appendix B. Likelihood ratios

Table B.3: Likelihood ratios calculated for item, from each group (105 items in total), for the proposition for membership of each group. Likelihood ratios using both log concave estimation, and kernel density estimation are given. The first row of this table is for a glass container with  $\Delta RI = 0.00214250$ . The likelihood ratio for that glass container being automotive glass calculated using log concave estimation is 0.0112, or moderate evidence that it was not automotive glass. The likelihood ratio for it being window glass is 0.00, which is highly compelling evidence against it being window glass, and the likelihood ratio for it being from a container is  $\approx 357$ , which is compelling evidence that it is from a container, which indeed it is. The final three columns give the likelihood ratios calculated using kernel density estimation, and can be interpreted in a similar manner to those likelihood ratios calculated using log-concave estimation.

item		Likelihood Ratio (log concave estimation)			Likelihood Ratio (kernel density estimation)		
glass category	$\Delta RI$	window	container	automotive	window	container	automotive
automotive	0.0021425	0.0112	0.00	357.38	$7.63 \times 10^{-4}$	$0.00 \times 10^{+0}$	$5.24 \times 10^{+3}$
automotive	0.0020350	0.0105	0.00	382.69	$2.70 \times 10^{-2}$	$2.10 \times 10^{-17}$	$1.48 \times 10^{+2}$
automotive	0.0019375	0.0173	0.00	231.87	$1.70 \times 10^{-1}$	$1.73 \times 10^{-17}$	$2.35 \times 10^{+1}$
automotive	0.0010900	1.3438	0.00	2.98	$0.00 \times 10^{+0}$	$2.23 \times 10^{-16}$	$1.80 \times 10^{+16}$
automotive	0.0010575	1.5881	0.00	2.52	$1.06 \times 10^{-18}$	$8.29 \times 10^{-16}$	$4.82 \times 10^{+15}$
automotive	0.0020450	0.0101	0.00	396.67	$2.24 \times 10^{-2}$	$1.00 \times 10^{-17}$	$1.79 \times 10^{+2}$
automotive	0.0018675	0.0247	0.00	161.81	$2.69 \times 10^{-1}$	$1.06 \times 10^{-16}$	$1.49 \times 10^{+1}$
automotive	0.0019150	0.0194	0.00	206.55	$2.06 \times 10^{-1}$	$4.81 \times 10^{-17}$	$1.95 \times 10^{+1}$
automotive	0.0020950	0.0106	0.00	376.01	$4.94 \times 10^{-3}$	$0.00 \times 10^{+0}$	$8.10 \times 10^{+2}$
automotive	0.0021575	0.0124	0.00	322.99	$3.10 \times 10^{-4}$	$0.00 \times 10^{+0}$	$1.29 \times 10^{+4}$
automotive	0.0018525	0.0267	0.00	149.81	$2.80 \times 10^{-1}$	$9.98 \times 10^{-18}$	$1.43 \times 10^{+1}$
automotive	0.0021350	0.0111	0.00	360.26	$1.02 \times 10^{-3}$	$0.00 \times 10^{+0}$	$3.93 \times 10^{+3}$
automotive	0.0018375	0.0288	0.00	138.69	$2.88 \times 10^{-1}$	$7.40 \times 10^{-17}$	$1.39 \times 10^{+1}$
automotive	0.0021775	0.0142	0.00	282.23	$1.19 \times 10^{-4}$	$0.00 \times 10^{+0}$	$3.36 \times 10^{+4}$
automotive	0.0019425	0.0168	0.00	237.90	$1.58 \times 10^{-1}$	$1.05 \times 10^{-16}$	$2.53 \times 10^{+1}$
automotive	0.0021050	0.0108	0.00	372.01	$3.00 \times 10^{-3}$	$7.66 \times 10^{-18}$	$1.33 \times 10^{+3}$
automotive	0.0020100	0.0119	0.00	336.55	$5.22 \times 10^{-2}$	$0.00 \times 10^{+0}$	$7.66 \times 10^{+1}$
automotive	0.0022750	0.0274	0.00	146.21	$7.00 \times 10^{-7}$	$0.00 \times 10^{+0}$	$5.71 \times 10^{+6}$
automotive	0.0018500	0.0270	0.00	147.89	$2.84 \times 10^{-1}$	$1.32 \times 10^{-17}$	$1.41 \times 10^{+1}$
automotive	0.0020425	0.0101	0.00	397.73	$2.24 \times 10^{-2}$	$1.00 \times 10^{-17}$	$1.79 \times 10^{+2}$
automotive	0.0019375	0.0173	0.00	231.87	$1.70 \times 10^{-1}$	$1.73 \times 10^{-17}$	$2.35 \times 10^{+1}$
automotive	0.0020150	0.0116	0.00	345.31	$4.48 \times 10^{-2}$	$0.00 \times 10^{+0}$	$8.92 \times 10^{+1}$
automotive	0.0020200	0.0113	0.00	354.30	$4.48 \times 10^{-2}$	$0.00 \times 10^{+0}$	$8.92 \times 10^{+1}$
automotive	0.0022175	0.0186	0.00	215.49	$2.22 \times 10^{-5}$	$0.00 \times 10^0$	$1.80 \times 10^{+5}$
automotive	0.0021150	0.0109	0.00	368.05	$2.31 \times 10^{-3}$	$8.90 \times 10^{-18}$	$1.73 \times 10^{+3}$
automotive	0.0011075	1.2282	0.00	3.26	$0.00 \times 10^{+0}$	$1.87 \times 10^{-16}$	$2.14 \times 10^{+16}$

Table B.3: (continued) likelihood ratios calculated for each item, for the propositions for membership of each group, modelled using both log-concave estimation, and kernel density estimation.

item		Likelihood Ratio (log concave estimation)			Likelihood Ratio (kernel density estimation)		
glass category	$\Delta RI$	window	container	automotive	window	container	automotive
automotive	0.0015200	0.1474	0.00	27.13	$3.19 \times 10^{-6}$	$8.79 \times 10^{-16}$	$1.26 \times 10^{+6}$
automotive	0.0019375	0.0173	0.00	231.87	$1.70 \times 10^{-1}$	$1.73 \times 10^{-17}$	$2.35 \times 10^{+1}$
automotive	0.0019300	0.0179	0.00	223.10	$1.82 \times 10^{-1}$	$5.24 \times 10^{-17}$	$2.19 \times 10^{+1}$
automotive	0.0020550	0.0102	0.00	392.45	$1.85 \times 10^{-2}$	$0.00 \times 10^{+0}$	$2.17 \times 10^{+2}$
automotive	0.0019550	0.0158	0.00	253.69	$1.34 \times 10^{-1}$	$7.45 \times 10^{-18}$	$2.99 \times 10^{+1}$
automotive	0.0019350	0.0175	0.00	228.91	$1.70 \times 10^{-1}$	$1.73 \times 10^{-17}$	$2.35 \times 10^{+1}$
window	-0.0009400	$\infty$	0.00	0.00	$2.01 \times 10^{+16}$	$1.48 \times 10^{-16}$	$5.14 \times 10^{-17}$
window	-0.0006175	$\infty$	0.00	0.00	$7.34 \times 10^{+15}$	$3.49 \times 10^{-16}$	$1.96 \times 10^{-16}$
window	-0.0009750	$\infty$	0.00	0.00	$1.39 \times 10^{+16}$	$1.85 \times 10^{-16}$	$1.02 \times 10^{-16}$
window	-0.0007475	$\infty$	0.00	0.00	$1.45 \times 10^{+16}$	$1.46 \times 10^{-16}$	$1.30 \times 10^{-16}$
window	0.0050275	$\infty$	0.00	0.00	$\infty$	$0.00 \times 10^{+0}$	$0.00 \times 10^{+0}$
window	-0.0002550	$\infty$	0.00	0.00	$4.13 \times 10^{+11}$	$9.68 \times 10^{-12}$	$0.00 \times 10^{+0}$
window	-0.0007400	$\infty$	0.00	0.00	$1.58 \times 10^{+16}$	$1.10 \times 10^{-16}$	$1.44 \times 10^{-16}$
window	-0.0008300	$\infty$	0.00	0.00	$4.66 \times 10^{+16}$	$2.55 \times 10^{-17}$	$6.04 \times 10^{-17}$
window	-0.0008475	$\infty$	0.00	0.00	$7.86 \times 10^{+16}$	$2.83 \times 10^{-17}$	$2.26 \times 10^{-17}$
window	-0.0007725	$\infty$	0.00	0.00	$2.37 \times 10^{+16}$	$1.22 \times 10^{-16}$	$4.66 \times 10^{-17}$
window	-0.0008625	$\infty$	0.00	0.00	$7.03 \times 10^{+16}$	$5.04 \times 10^{-17}$	$6.56 \times 10^{-18}$
window	-0.0008550	$\infty$	0.00	0.00	$4.22 \times 10^{+16}$	$7.43 \times 10^{-17}$	$2.05 \times 10^{-17}$
window	-0.0010225	$\infty$	0.00	0.00	$8.36 \times 10^{+15}$	$3.88 \times 10^{-16}$	$9.02 \times 10^{-17}$
window	-0.0008625	$\infty$	0.00	0.00	$7.03 \times 10^{+16}$	$5.04 \times 10^{-17}$	$6.56 \times 10^{-18}$
window	-0.0009000	$\infty$	0.00	0.00	$6.34 \times 10^{+16}$	$6.31 \times 10^{-17}$	$0.00 \times 10^{+0}$
window	-0.0007675	$\infty$	0.00	0.00	$1.82 \times 10^{+16}$	$1.66 \times 10^{-16}$	$5.33 \times 10^{-17}$
window	-0.0017300	$\infty$	0.00	0.00	$1.82 \times 10^{+15}$	$1.03 \times 10^{-16}$	$2.10 \times 10^{-15}$
window	-0.0007400	$\infty$	0.00	0.00	$1.58 \times 10^{+16}$	$1.10 \times 10^{-16}$	$1.44 \times 10^{-16}$
window	-0.0008625	$\infty$	0.00	0.00	$7.03 \times 10^{+16}$	$5.04 \times 10^{-17}$	$6.56 \times 10^{-18}$
window	-0.0010425	$\infty$	0.00	0.00	$1.42 \times 10^{+16}$	$2.12 \times 10^{-16}$	$6.92 \times 10^{-17}$
window	-0.0009475	$\infty$	0.00	0.00	$1.76 \times 10^{+16}$	$1.46 \times 10^{-16}$	$8.07 \times 10^{-17}$
window	-0.0010150	$\infty$	0.00	0.00	$5.86 \times 10^{+16}$	$2.02 \times 10^{-17}$	$4.80 \times 10^{-17}$
window	0.0018925	0.0217	0.00	183.99	$2.46 \times 10^{-1}$	$8.46 \times 10^{-17}$	$1.62 \times 10^{+1}$
container	0.0002100	0.0957	41.79	0.00	$8.71 \times 10^{-11}$	$4.59 \times 10^{+10}$	$1.34 \times 10^{-17}$
container	0.0002150	0.0942	42.47	0.00	$8.71 \times 10^{-11}$	$4.59 \times 10^{+10}$	$1.34 \times 10^{-17}$
container	0.0001767	0.1067	37.49	0.00	$1.69 \times 10^{-9}$	$2.37 \times 10^{+9}$	$6.33 \times 10^{-17}$
container	0.0001000	0.1554	25.75	0.00	$1.24 \times 10^{-6}$	$3.24 \times 10^{+6}$	$8.85 \times 10^{-17}$
container	0.0001817	0.1050	38.10	0.00	$9.43 \times 10^{-10}$	$4.24 \times 10^{+9}$	$6.46 \times 10^{-17}$
container	0.0001367	0.1298	30.81	0.00	$4.83 \times 10^{-8}$	$8.29 \times 10^{+7}$	$3.89 \times 10^{-17}$
container	0.0000883	0.1733	23.08	0.00	$2.12 \times 10^{-6}$	$1.89 \times 10^{+6}$	$7.31 \times 10^{-17}$
container	0.0001317	0.1330	30.07	0.00	$8.25 \times 10^{-8}$	$4.85 \times 10^{+7}$	$2.02 \times 10^{-17}$
container	0.0001233	0.1386	28.87	0.00	$1.42 \times 10^{-7}$	$2.81 \times 10^{+7}$	$3.08 \times 10^{-17}$
container	0.0001433	0.1256	31.84	0.00	$2.81 \times 10^{-8}$	$1.43 \times 10^{+8}$	$2.18 \times 10^{-17}$
container	0.0002650	0.1201	33.31	0.00	$6.49 \times 10^{-13}$	$6.16 \times 10^{+12}$	$1.08 \times 10^{-16}$
container	0.0002217	0.0973	41.12	0.00	$4.75 \times 10^{-11}$	$8.43 \times 10^{+10}$	$2.65 \times 10^{-17}$

Table B.3: (continued) likelihood ratios calculated for each item, for the propositions for membership of each group, modelled using both log-concave estimation, and kernel density estimation.

item		Likelihood Ratio (log concave estimation)			Likelihood Ratio (kernel density estimation)		
glass category	$\Delta RI$	window	container	automotive	window	container	automotive
container	0.0000900	0.1632	24.52	0.00	$2.12 \times 10^{-6}$	$1.89 \times 10^{+6}$	$7.31 \times 10^{-17}$
container	0.0002600	0.1172	34.13	0.00	$1.20 \times 10^{-12}$	$3.34 \times 10^{+12}$	$1.44 \times 10^{-16}$
container	0.0000933	0.1605	24.92	0.00	$2.12 \times 10^{-6}$	$1.89 \times 10^{+6}$	$7.31 \times 10^{-17}$
container	0.0004300	0.3698	10.82	0.00	$8.36 \times 10^{-17}$	$8.10 \times 10^{+15}$	$4.11 \times 10^{-16}$
container	0.0000767	0.2642	15.14	0.00	$6.29 \times 10^{-6}$	$6.36 \times 10^{+5}$	$5.52 \times 10^{-17}$
container	0.0002150	0.0942	42.47	0.00	$8.71 \times 10^{-11}$	$4.59 \times 10^{+10}$	$1.34 \times 10^{-17}$
container	0.0001750	0.1076	37.18	0.00	$1.69 \times 10^{-9}$	$2.37 \times 10^{+9}$	$6.33 \times 10^{-17}$
container	0.0003350	0.1687	23.70	0.00	$6.67 \times 10^{-16}$	$5.15 \times 10^{+15}$	$1.11 \times 10^{-16}$
container	0.0001550	0.1187	33.71	0.00	$9.31 \times 10^{-9}$	$4.30 \times 10^{+8}$	$6.10 \times 10^{-17}$
container	0.0001617	0.1148	34.83	0.00	$5.30 \times 10^{-9}$	$7.54 \times 10^{+8}$	$5.46 \times 10^{-17}$
container	0.0001067	0.1504	26.60	0.00	$7.21 \times 10^{-7}$	$5.55 \times 10^{+6}$	$8.25 \times 10^{-17}$
container	0.0002883	0.1345	29.74	0.00	$9.71 \times 10^{-14}$	$4.11 \times 10^{+13}$	$1.97 \times 10^{-16}$
container	0.0000267	1.6117	2.48	0.00	$3.09 \times 10^{-4}$	$1.30 \times 10^{+04}$	$1.71 \times 10^{-16}$
container	0.0001783	0.1061	37.69	0.00	$1.69 \times 10^{-9}$	$2.37 \times 10^{+9}$	$6.33 \times 10^{-17}$
container	0.0002533	0.1135	35.25	0.00	$2.19 \times 10^{-12}$	$1.83 \times 10^{+12}$	$9.73 \times 10^{-17}$
container	0.0002283	0.1005	39.81	0.00	$2.58 \times 10^{-11}$	$1.55 \times 10^{+11}$	$5.54 \times 10^{-17}$
container	0.0001833	0.1044	38.31	0.00	$9.43 \times 10^{-10}$	$4.24 \times 10^{+9}$	$6.46 \times 10^{-17}$
container	0.0003450	0.1772	22.58	0.00	$6.72 \times 10^{-17}$	$1.89 \times 10^{+16}$	$1.45 \times 10^{-16}$
container	0.0003600	0.1905	20.99	0.00	$0.00 \times 10^{+0}$	$1.75 \times 10^{+16}$	$2.28 \times 10^{-16}$
container	0.0002817	0.1302	30.72	0.00	$1.85 \times 10^{-13}$	$2.16 \times 10^{+13}$	$1.47 \times 10^{-16}$
container	0.0001000	0.1554	25.75	0.00	$1.24 \times 10^{-6}$	$3.24 \times 10^{+6}$	$8.85 \times 10^{-17}$
container	0.0001767	0.1067	37.49	0.00	$1.69 \times 10^{-9}$	$2.37 \times 10^{+9}$	$6.33 \times 10^{-17}$
container	0.0003033	0.1447	27.65	0.00	$2.55 \times 10^{-14}$	$1.57 \times 10^{+14}$	$4.56 \times 10^{-17}$
container	0.0001500	0.1216	32.89	0.00	$1.62 \times 10^{-8}$	$2.47 \times 10^{+8}$	$7.38 \times 10^{-17}$
container	0.0002500	0.1116	35.83	0.00	$2.19 \times 10^{-12}$	$1.83 \times 10^{+12}$	$9.73 \times 10^{-17}$
container	0.0003117	0.1507	26.55	0.00	$6.25 \times 10^{-15}$	$6.26 \times 10^{+14}$	$1.44 \times 10^{-16}$
container	0.0003133	0.1519	26.34	0.00	$6.25 \times 10^{-15}$	$6.26 \times 10^{+14}$	$1.44 \times 10^{-16}$
container	0.0002367	0.1046	38.23	0.00	$7.54 \times 10^{-12}$	$5.31 \times 10^{+11}$	$7.37 \times 10^{-17}$
container	0.0002233	0.0981	40.79	0.00	$2.58 \times 10^{-11}$	$1.55 \times 10^{+11}$	$5.54 \times 10^{-17}$
container	0.0003600	0.1905	20.99	0.00	$0.00 \times 10^{+0}$	$1.75 \times 10^{+16}$	$2.28 \times 10^{-16}$
container	0.0004000	0.2754	14.52	0.00	$1.33 \times 10^{-17}$	$1.08 \times 10^{+16}$	$3.58 \times 10^{-16}$
container	0.0003650	0.1952	20.49	0.00	$0.00 \times 10^{+0}$	$1.58 \times 10^{+16}$	$2.54 \times 10^{-16}$
container	0.0001367	0.1298	30.81	0.00	$4.83 \times 10^{-8}$	$8.29 \times 10^{+7}$	$3.89 \times 10^{-17}$
container	0.0003700	0.2051	19.51	0.00	$0.00 \times 10^{+0}$	$1.58 \times 10^{+16}$	$2.54 \times 10^{-16}$
container	0.0002483	0.1107	36.12	0.00	$4.05 \times 10^{-12}$	$9.87 \times 10^{+11}$	$6.08 \times 10^{-17}$
container	0.0002250	0.0989	40.46	0.00	$2.58 \times 10^{-11}$	$1.55 \times 10^{+11}$	$5.54 \times 10^{-17}$
container	0.0002000	0.0989	40.45	0.00	$2.89 \times 10^{-10}$	$1.38 \times 10^{+10}$	$6.06 \times 10^{-17}$
container	0.0002117	0.0952	42.02	0.00	$8.71 \times 10^{-11}$	$4.59 \times 10^{+10}$	$1.34 \times 10^{-17}$

Table 2: Percentage likelihood ratios from each glass category, and their negations, calculated using log-concave estimation and kernel density estimation. Each cell is the percentage of likelihood ratios falling within the likelihood ratio range given by the column. For example, the first row are for likelihood ratios calculated using log-concave estimation for those glasses known to come from windows for the proposition that those glass items were from window glass. 4% of those likelihood ratios were between  $10^{-2} - 10^{-1}$ , and 96% were  $> 10^5$ . In this case the expectation is that the likelihood ratios will be large, and more specifically the likelihood ratios will be greater than one. In this case one might say that the 4% of likelihood ratios which are less than one might form misleading evidence as to the source of those glass objects. The second row is for glass objects known to be from windows, but for the proposition that those glasses were in fact from automobiles or containers. Here we expect small likelihood ratios, ideally less than one. Here 44% were between  $10^{-2}$  and  $10^{-1}$ , and 51% between  $10^{-1}$  and 1. However, 5% of the likelihood ratios were between 1 and 10, which again, would be misleading evidence, although not very strong misleading evidence. Empty cells indicate the value zero.

likelihood ratio		$0 - 10^{-5}$	$10^{-5} - 10^{-4}$	$10^{-4} - 10^{-3}$	$10^{-3} - 10^{-2}$	$10^{-2} - 10^{-1}$	$10^{-1} - 10^0$	$10^0 - 10^1$	$10^1 - 10^2$	$10^2 - 10^3$	$10^3 - 10^4$	$10^4 - 10^5$	$> 10^5$
log-concave estimation	window					4							96
	not window					44	51	5					
	container							2	98				
	not container	100											
	automotive							9	3	88			
	not automotive	99								1			
density estimation	window						4						96
	not window	66	1	5	5	9	15						
	container											2	98
	not container	100											
	automotive							47	16	12	6	19	
	not automotive	99						1					